J Fluoresc
DOI 10.1007/s10895-008-0345-y

ORIGINAL PAPER

On Mechanism of Intermediate-Sized Circular DNA Compaction Mediated by Spermine: Contribution of Fluorescence Lifetime Correlation Spectroscopy

Jana Humpolíčková · Miroslav Štěpánek · Teresa Kral · Aleš Benda · Karel Procházka · Martin Hof

Received: 31 October 2007 / Accepted: 30 January 2008
© Springer Science + Business Media, LLC 2008

Abstract The compaction of DNA plays a role in the nuclei of several types of cells and becomes important in the non-viral gene therapy. Thus, it is in the scope of research interest. It was shown, that spermine-induced compaction of large DNA molecules occurs in a discrete "all-or-non" regime, where the coexistence of free and folded DNA molecules was observed. In the case of intermediate-sized DNA molecules (~10 kbp), so far, it was stated that the mechanism of folding is continuous. Here, we show, that neither a standard benchmark technique—dynamic light scattering, nor a single molecule technique such as fluorescence correlation spectroscopy, can decide what kind of mechanism is undertaken in the compaction process. Besides, we introduce an application of a new approach—fluorescence lifetime correlation spectroscopy. The method takes an advantage of a subtle lifetime change of an intercalating dye PicoGreen® during the titration with spermine and based on that, it reveals the discrete mechanism of the process. Furthermore, we show that it allows for observation of the equilibrium state transition dynamics.

Keywords DNA compaction · Fluorescence correlation spectroscopy · Fluorescence lifetime correlation spectroscopy · Dynamic light scattering

J. Humpolíčková · T. Kral · A. Benda · M. Hof (✉)
J. Heyrovský Institute of Physical Chemistry,
Academy of Sciences of the Czech Republic,
Dolejškova 3,
182 23 Prague 8, Czech Republic
e-mail: Hof@jh-inst.cas.cz

M. Štěpánek · K. Procházka
Department of Physical and Macromolecular Chemistry
and Laboratory of Specialty Polymers, School of Science,
Charles University in Prague,
Albertov 2030,
128 40 Prague 2, Czech Republic

T. Kral
Department of Physics and Biophysics, Agricultural University,
Norwida 25,
50-375 Wrocław, Poland

Introduction

In viruses, bacteria, prokaryotes, and sperm cells, the DNA chain is packed into extremely dense structures by polyamine molecules such as spermine (4+) or spermidine (3+). Such a tightly packed state is used in living systems for storage of long DNA molecules. The biologically relevant in-vitro system for such DNA packaging of single DNA molecules is called DNA compaction, which can be generated by a variety of multivalent cations [1]. There is an impressive amount of studies characterizing the morphology of the compacted DNA state by cryoelecton microscopy and it appears to be possible to rationalize the conditions for forming toroids, spherical globules, rods, or rackets [2]. While "ensemble" methods like dynamic light scattering [3], small angle neutron scattering [4], or photon correlation spectroscopy [5] indicated that DNA compaction should be considered as a continuous process, Yoshikawa's microscopy observations allowing to visualize large single DNA molecules (166 kbp) for the first clearly demonstrated the discrete ("non-or-all") character of the DNA coil–globule transition [6]. The same group could visualize the compaction by fluorescence microscopy directly in real time [7]. It was shown that a compact part on the 166 kbp DNA chain appears and grows within several seconds until complete collapse. In most cases, it is the initial formation of loops or bundles which leads to the

compact structures. These intermediate conformations are transformed kinetically into a final, fully compact state. Recent studies on compaction showed that under certain conditions, addition of aminated PEG [8], H1 histone proteins [9], hydrophobic dications [10], pteridine–polyamine conjugates [11], synthetic polyelectrolytes [12], and ascorbic acid [13] to giant DNA chains (58 to 166 kbp) induced unfolded and compact phases of DNA coexisting along a *single* DNA molecule. It is important to note, that all these mechanistic observation based on fluorescence microscopy were done using rather large DNA molecules. For example for the bacteriophage T4 DNA (166 kbp), which was preferentially used by the above mentioned studies by Yoshikawa, a hydrodynamic radius of about 900 nm and 90 nm was determined for the unfolded and spermine-induced compacted state, respectively [14].

In a recent study [15], the same group for the first time applied fluorescence microscopy together with a Brownian motion analysis on the spermine-induced compaction of circular plasmide of an intermediate size (12.5 kbp). In contrast to those large linear DNA molecules larger than several tens of kilobase pairs, the authors found a comparable small change of the hydrodynamic radius from the elongated form (260 nm) to about 150 nm in the compact state and characterized the folding transition as continuous. Up to our knowledge, this study is the only single-molecule observation of compaction of a non-adsorbed, freely diffusing circular plasmide of an intermediate size. Taking into account the physiological relevance of such "small" DNA structures [15] and the fact that the resolution of usual fluorescence microscopy is diffraction-limited, there is certainly a need for applying alternative techniques which are able to monitor the spermine-DNA interaction in solution on a single molecule level.

Fluorescence correlation spectroscopy (FCS) is a microscopic technique that analysis fluorescence fluctuations arising from the diffusion of fluorescently labeled species in and out of the diffraction limited (femtoliter sized) confocal volume. It generally provides information on the diffusion coefficient of fluorescently labeled species [16]. Since DNA compaction leads to a dramatic change in the hydrodynamic radius, FCS seems to be predestinated for the investigation of these processes, especially for DNA sizes where the interpretation of single molecule fluorescence microscopy images is not straightforward. In this article, the use of confocal FCS for characterization of DNA compaction is illustrated by spermine titration of a PicoGreen® (PG)-labeled circular 10 kbp DNA, in a similar way as already demonstrated earlier [17–19]. We show, that despite the changes in typical FCS read-out parameters are rather steep and thus suggesting a step-like compaction process, they do not suggest whether it is continuous or discrete. Apart from that, we demonstrate that even a dynamic light scattering—a standard benchmark technique, can not resolve coexistence of free and compact DNA molecules during the folding process.

Beside of monitoring the classical FCS read-out parameters, we simultaneously monitor spermine-induced changes in the fluorescence lifetime by using pulsed laser excitation and the so-called time-tagged time-resolved (TTTR) data storage mode [20]. An advantage of this approach is that from a single measurement we simultaneously obtain information on the molecule microenvironment (carried in the fluorescence lifetime) and its diffusion properties (obtained by confocal FCS).

Finally, a combination of FCS and simultaneous fluorescence lifetime acquisition resulted into an application of a rather new technique fluorescence lifetime correlation spectroscopy (FLCS) [21–24]. While FCS provides information on mean residence time of particles in the focus and consequently, on their diffusion coefficient, FLCS additionally distinguishes between fluorophores with different lifetimes and similarly to dual-color FCS [25], enables to calculate cross-correlation functions between two particles of different fluorescent lifetimes and thus reveals interactions between them. In this particular case, we demonstrate that FLCS allows for distinguishing whether the spermine induced folding of PicoGreen® (PG)-labeled circular 10 kbp DNA occurs in a continuous or discrete way, thus the new insights into a so far unsolved problem are given.

Materials and methods

DNA samples and labeling

The 10 kbp pH βApr-1-Neo plasmid was a gift from the laboratory of Prof. Maciej Ugorski (Ludwik Hirszfeld Institute of Immunology and Experimental Therapy, Wrocław, Poland). It was prepared as described elsewhere [26] with slight modifications during the final purification stage [27]. PicoGreen® was purchased from Molecular Probes (Leiden, The Netherlands) and spermine from Sigma. We used the labeling ratio 1 PG/100 basepairs. Experiments were performed in a TE buffer (pH 7.95, 10 mM Tris, 1 mM EDTA) at room temperature (25 °C).

Instrumental setup

FLCS measurements were performed on a MicroTime 200 inverted confocal microscope (PicoQuant, Germany). We used a pulsed diode laser (LDH-P-C-470, 470 nm, PicoQuant) providing 80 ps pulses at 40 MHz repetition rate, dichroic mirror 490 DRLP and band-pass filter 515/50 (Omega Optical), and a water immersion objective (1.2 NA, 60x) (Olympus). Low power of 4 μW (at the back aperture

of the objective) was chosen to minimize photobleaching and saturation [28]. In the detection plane, a pinhole (50 μm in diameter) was used and the signal was subsequently splitted on two single photon avalanche diodes (SPADs, PDMs, Microphoton Devises, Bolzano, Italy). For calculating fluorescence correlation curves, we correlated only photons from different SPADs to prevent detector afterpulsing.

Data acquisition and processing

Photon arrival times were stored using fast electronics (Picoharp 300, PicoQuant) in time-tagged time-resolved recording mode. Every detected photon was assigned (1) a time after the beginning of the measurement and (2) a time after the previous laserpulse. All the data were acquired for 2 h in order to achieve good photon statistics. The FLCS data analysis was done using home built routines (DevC++, Bloodshed Software and OriginPro70, OriginLab Corporation).

Dynamic light scattering

The light scattering setup (ALV, Langen, Germany) consisted of a 633 nm He–Ne laser, an ALV CGS/8F goniometer, an ALV High QE APD detector, and ALV 5000/EPP multibit, multitau autocorrelator. The measurements were performed at the scattering angle θ=90°. Prior to measurement, samples were filtered through 0.45 μm Acrodisc filters.

The DLS data analysis was performed by fitting the normalized intensity autocorrelation function, $g^{(2)}(\tau)$, to the equation

$$g^{(2)}(\tau) = 1 + \beta\left[\int_0^\infty A(\tau_R)\exp\left(-\frac{\tau}{\tau_R}\right)d\tau_R\right]^2, \qquad (1)$$

where β is a factor accounting for deviation from the ideal correlation and $A(\tau_R)$ is the distribution function of relaxation times τ_R. The fitting procedure, providing the relaxation time distribution, was based on the Inverse Laplace Transform (ILT) with the aid of a constrained regularization algorithm (CONTIN).

Results and discussion

Confocal FCS on free DNA

Since the size of DNA exceeds three times the diameter of the laser focus, the autocorrelation curve (ACF) for multiply labeled DNA molecules are difficult to model. The segmental motion and the Brownian motion of the whole molecule are superimposed, which typically causes additional fluctuations lowering the amplitude of ACFs and increases the apparent number of particles in the focus. For the sake of simplicity, the ACF of free DNA was fitted to a model taking into account one freely diffusing species in the detection volume:

$$G(\tau) = 1 + \frac{1}{PN(1-T)}\left(1 - T\left(1 - e^{-\frac{\tau}{\tau_0}}\right)\right) \cdot \left(\frac{1}{1+(\tau/\tau_{res})} \cdot \frac{1}{\left(1+(\tau/\tau_{res})(\omega_0/\omega_Z)^2\right)^{\frac{1}{2}}}\right) \qquad (2)$$

Being aware of the complexity of DNA movement, we assign the residence time τ_{res} to the lateral movement of the whole molecule. The triplet-like term containing the "triplet" parameters T and τ_0 describe here the effect of the segmental motion of the chain [29] and are specific for our DNA. PN is an apparent number of particles in the detection volume. ω_0 and ω_Z are half axes of that detection volume. Although Eq. 2 has a rather empirical character, it is totally sufficient for our purposes.

Compaction with different amounts of spermine—FCS approach

FCS experiments with increasing spermine concentration were performed and the FCS fit parameters followed (see Fig. 1).

At first, we observe almost no change in τ_{res} and PN. As already reported in [14], at these ratios, sodium ions in minor grooves [30] are replaced by molecules of spermine. During this exchange, the simultaneously measured fluorescence lifetime of PG does not change either, which means that the dye "sees" the same microenvironment. At a

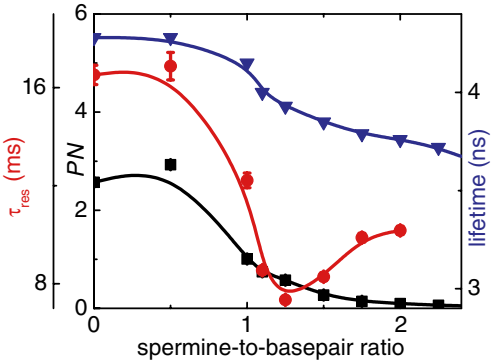

Fig. 1 Dependence of particle number (*squares*), residence time (*circles*) and lifetime (*triangles*) on spermine-to-basepair ratio. Concentration of DNA was 1 nmol/l

spermine-to-basepair ratio close to one, τ_{res} decreases as well as *PN* and the lifetime. This moment corresponds to the folding of the DNA molecules that reached the complete neutralization. The drop in *PN* shows that folded DNA resembles a rigid point-like molecule much smaller than the size of the detection volume [31] and thus, inner motions no longer contribute to the FCS signal. The lifetime drop refers to the changed microenviroment of PG [32]. After sufficient accumulation of condensed DNA molecules, the condensed DNA starts to aggregate, which causes heterogeneity in the correlation curves, a prolongation of τ_{res} and a further *PN* decrease. The lifetime remains constant as the additional aggregation does not change the immediate microenvironment of PG. In summary, all three parameters (τ_{res}, *PN*, and lifetime) reflect the process of DNA compaction.

Compaction with different amounts of spermine—dynamic light scattering

The same experiment was followed also via dynamic light scattering. Figure 2 shows the distribution of relaxation times upon adding different amounts of spermine. Obviously, the mean relaxation time shifts to the lower values at higher spermine-to-basepair ratios. In the case of free DNA, we can additionally observe a faster mode corresponding to the rotational or internal motions [33, 34] of the semiflexible DNA chain. It is worth noticing that the width of the distribution passes a maximum during the dependence on the spermine-to-basepair ratio. Since the relaxation times of the free and folded DNA are not enough separated, it can not be decided whether the broadening arises from coexistence of two subpopulations or merely from a broader population of DNA molecules in different stages of the compaction.

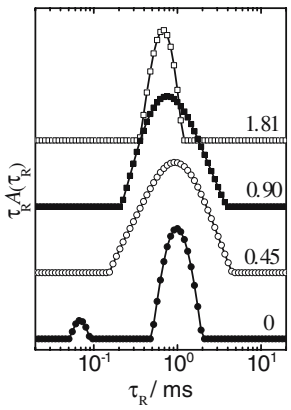

Fig. 2 Intensity weighted distribution functions of relaxation times obtained from the dynamic light scattering experiment for different spermine-to-basepair ratios: 0, 0.45, 0.90, 1.81. Concentration of DNA was 1 nmol/l

Thus, neither from the FCS experiments, nor from the light scattering data, it can be decided whether the DNA molecules collapse in the discrete "non-or-all" regime or whether the change is continuous.

Fluorescence lifetime correlation spectroscopy

Fluorescence lifetime correlation spectroscopy (FLCS) [24] was designed similarly as dual-color FCS for the multicomponent analysis. While dual-color FCS takes the advantage of different emission properties of different fluorescent species, FLCS employs fluorescence lifetimes for distinguishing between individual chromophores. Since the lifetime is a parameter that is often sensitive to the microenvironment, FLCS also brings the opportunity to calculate autocorrelation curves for single dye in two different locations [23]. Moreover, it provides cross-correlation functions (CCFs) as well, which enables to reveal interactions between the locations of the probe, i.e. aggregate formation or state dynamics.

Compared to the dual-color FCS, FLCS does not need more lasers and more detection paths, the only requirements are pulsed laser and a card allowing for the special data storage mode. Each detected photon is assigned a macroscopic arrival time t, which is the time that elapsed since the start of the measurement (microsecond resolution) and a microscopic time, which is the time elapsed since the previous laser pulse (nanosecond resolution). The microscopic time is described by a discrete channel number j.

At every macroscopic arrival time t, the fluorescence intensity $I_j(t)$ in each channel j is a linear combination of normalized fluorescence histograms p_j^k:

$$I_j(t) = \sum_{k=1}^{n} w^k(t) p_j^k \tag{3}$$

where k stands for a particular emitter with a specific fluorescence decay, n is the number of different emitters with different fluorescence decays and $w^k(t)$ is the contribution of the k^{th} fluorescent species to the total fluorescence signal.

Equation 3 is an over-determined set of linear equations. Assuming that the photon detection obeys a Poissonian distribution and applying singular value decomposition, the solution of the Eq. 3 can be written as follows:

$$w^k(t) = \sum_{j=1}^{N} f_j^k I_j(t), \tag{4}$$

where N is the number of channels and f_j^k is a discrete filter function, which is constructed from the fluorescence decay histograms of the different fluorescence species and the

total intensity of the compound signal. Explicitly, f_j^k is given by:

$$f_j^k = \left(\left[\widehat{M}^T \cdot \mathrm{diag}\langle I_j(t) \rangle_t^{-1} \cdot \widehat{M} \right]^{-1} \cdot \widehat{M}^T \cdot \mathrm{diag}\langle I_j(t) \rangle_t^{-1} \right)_{kj}, \tag{5}$$

where the matrix elements are:

$$\widehat{M}_{jk} = p_j^k. \tag{6}$$

Finally, the auto- ($k=l$) and cross-correlation ($k \neq l$) functions are calculated as:

$$G^{kl}(\tau) = \frac{\sum_{i=1}^{N} \sum_{j=1}^{N} f_i^k f_j^l \langle I_i(t) I_j(t+\tau) \rangle_t}{\sum_{i=1}^{N} \sum_{j=1}^{N} f_i^k f_j^l \langle I_i(t) \rangle_t \langle I_j(t) \rangle_t} \tag{7}$$

FLCS revealing mechanism of DNA compaction

Here, we focus on the middle point of the titration experiment, where the spermine-to-basepair ratio equals 1, i.e. before the entire relaxation takes place. It can be shown, that the decay of the middle point is a linear combination of the decay patterns of free and compact DNA measured separately and of uniform noise. Following situations can be expected:

1. DNA compaction is a continuous process: all the DNA molecules start to form condensed regions, where the lifetime of PG is shortened, i.e., DNA contains both 4.2-ns (4-ns for short) and 3.5-ns (3-ns for short) lifetime fluorophores. In this case, the ACF of the 4-ns lifetime component decays at shorter lag-times compared to the ACF of free DNA and vice versa, the ACF of the 3-ns lifetime component decays at longer lag-times compared to the ACF of the condensed DNA. The non-one CCFs appear.
2. DNA compaction is a discrete "all-or-none" process: DNA molecules coexist in the uncondensed and in the condensed form. In this case, the ACF of the 4-ns lifetime component matches the ACF of the free DNA and the ACF of the 3-ns lifetime component matches the ACF of the condensed DNA. No cross-correlation is expected.

Comparison of the ACFs depicted in the Fig. 3 clearly shows that the later case is the correct one, i.e. the compaction is a discrete transition. The non-one CCFs suggest, however, that apart from the majority of the molecules that are in one of the states, there is a fraction of molecules bearing both the 3- and 4-ns lifetime components. Based on the fact that the amplitudes of the CCFs are between the amplitudes of the ACFs, it can be concluded that there is not only a static coexistence of the domains, but a dynamic equilibrium transition between them. More detailed inspection of the CCFs is given in [34].

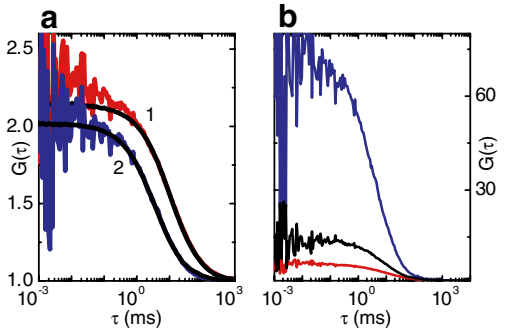

Fig. 3 **a** Noisy curves 1 and 2: particle number corrected ACFs of the 4- and 3-ns lifetime component obtained from the measurement of the middle point, respectively. Corresponding smooth curves: Particle number normalized ACFs obtained for unfolded DNA (*curve 1*) and folded DNA (*curve 2*) measured separately. **b** From the lowest amplitude to the highest: ACF of the 4-ns lifetime component, CCF between 3- and 4-ns component, ACF of the 4-ns lifetime component obtained from the measurement of the middle point, respectively

Conclusion

In this contribution, we show that FCS as well as the light scattering are good tools to study compaction of DNA induced by spermine. Both the approaches show a steep change of the read-out parameters corresponding to the conformational change of DNA molecules. Neither FCS, nor light scattering, however, can give a closer insight into the mechanism of the condensation, i.e., resolve whether the compaction is a continuous or a discrete all-or-non transition.

We introduce a brand new technique FLCS that allows to characterize diffusion properties of species differing in lifetime. Based on the fact that PG has a different lifetime in the folded and unfolded domains of the DNA molecule, FLCS allows for a detailed insight into the middle point of the DNA titration by spermine. The comparison of the ACFs obtained for the both the lifetime components present in the middle point with ACFs of free and compact DNA clearly reveals that the compaction of the intermediate-sized 10 kbp circular DNA molecule occur in the all-or-non regime. There is only a small fraction of molecules (not observable in ACFs) that contain both the 3- and 4-ns labeled domains. These molecules are responsible for the CCFs curves, suggesting not only a static coexistence of the domains but an equilibrium interchange between the folded and unfolded ones.

Acknowledgement We acknowledge support of the Ministry of Education of the Czech Republic via grant LC06063 (JH, AB, MH) and long-term research project MSM0021620857 (MŠ, KP) and the Academy of Sciences of the Czech Republic via grant IAA400400621 (TK, MŠ).

References

1. Bloomfield VA (1996) Curr Opin Struct Biol 6(3):334–341
2. Zinchenko AA, Baigl D, Yoshikawa K (2007) In: Nalwa HS (ed) Polymeric Nanostructures and their Applications. American Scientific Publishers, Valencia
3. Yu JQ, Wang ZL, Chu B (1992) Macromolecules 25(5):1618–1620
4. Nierlich M, Cotton JP, Farnoux B (1978) J Chem Phys 69 (4):1379–1383
5. Sun ST, Nishio I, Swislow G, Tanaka T (1980) J Chem Phys 73 (12):5971–5975
6. Yoshikawa K, Takahashi M, Vasilevskaya VV, Khokhlov AR (1996) Phys Rev Lett 76(16):3029–3031
7. Yoshikawa K, Matsuzawa Y (1996) J Am Chem Soc 118(4):929–930
8. Yoshikawa K, Yoshikawa Y, Koyama Y, Kanbe T (1997) J Am Chem Soc 119(28):6473–6477
9. Yoshikawa Y, Velichko YS, Ichiba Y, Yoshikawa K (2001) Eur J Biochem 268(9):2593–2599
10. Zinchenko AA, Sergeyev VG, Murata S, Yoshikawa K (2003) J Am Chem Soc 125(15):4414–4415
11. Chen N, Zinchenko AA, Murata S, Yoshikawa K (2005) J Am Chem Soc 127(31):10910–10916
12. Kiriy A, Gorodyska G, Minko S, Jaeger W, Stepanek P, Stamm M (2002) J Am Chem Soc 124(45):13454–13462
13. Yoshikawa Y, Suzuki M, Chen N, Zinchenko AA, Murata S, Kanbe T, Nakai T, Oana H, Yoshikawa K (2003) Eur J Biochem 270(14):3101–3106
14. Makita N, Yoshikawa K (2002) Biophys Chem 99(1):43–53
15. Satoa YT, Hamada T, Kubo K, Yamada A, Kishida T, Mazda O, Yoshikawa K (2005) FEBS Lett 579(14):3095–3099
16. Thompson NL, Lieto AM, Allen NW (2002) Curr Opin Struct Biol 12(5):634–641
17. Kral T, Langner M, Benes M, Baczynska D, Ugorski M, Hof M (2002) Biophys Chem 95(2):135–144
18. Kral T, Widerak K, Langner M, Hof M (2005) J Fluoresc 15 (2):179–183
19. Kral T, Langner M, Hof M (2006) Chemotherapy 52(4):196–199
20. Kapusta P, Wahl M, Benda A, Hof M, Enderlein J (2007) J Fluoresc 17(1):43–48
21. Bohmer M, Wahl M, Rahn HJ, Erdmann R, Enderlein J (2002) Chem Phys Lett 353(5–6):439–445
22. Benda A, Hof M, Wahl M, Patting M, Erdmann R, Kapusta P (2005) Rev Sci Instrum 76(3):033106
23. Benda A, Fagul'ova V, Deyneka A, Enderlein J, Hof M (2006) Langmuir 22(23):9580–9585
24. Gregor I, Enderlein J (2007) Photochem Photobiol Sci 6(1):13–18
25. Schwille P, MeyerAlmes FJ, Rigler R (1997) Biophys J 72 (4):1878–1886
26. Sombrook J, Fritsch EF, Maniatis T (1989) In: Cold Spring Harbor Laboratory Press, New York
27. Kral T, Hof M, Langner M (2002) Biol Chem 383(2):331–335
28. Gregor I, Patra D, Enderlein J (2005) ChemPhysChem 6(1):164–170
29. Winkler RG, Keller S, Radler JO (2006) Phys Rev E 73 (4):041919
30. Korolev N, Lyubartsev AP, Laaksonen A, Nordenskiold L (2002) Biophys J 82(6):2860–2875
31. Adjimatera N, Kral T, Hof M, Blagbrough IS (2006) Pharm Res 23(7):1564–1573
32. Schweitzer C, Scaiano JC (2003) Phys Chem Chem Phys 5 (21):4911–4917
33. Seils J, Pecora R (1995) Macromolecules 28(3):661–673
34. Humpolickova J, Benda A, Sykora J, Machan R, Kral T, Gasinska B, Enderlein J, Hof M (2008) Biophys J 94(3):L17–L19